SPANDIDOS PUBLICATIONS

MOLECULAR MEDICINE REPORTS 19: 499-507, 2019

Function of BRD4 in the pathogenesis of high glucose-induced cardiac hypertrophy

QIAN WANG[1], YUXIN SUN[2], TIANSHU LI[3], LIANQIN LIU[1], YUNXIA ZHAO[1], LIYUAN LI[1], LING ZHANG[1] and YAN MENG[1]

[1]Department of Pathophysiology, Prostate Diseases Prevention and Treatment Research Center, College of Basic Medical Science; [2]Department of Otorhinolaryngology, China-Japan Union Hospital; [3]Department of Functional Science Experiment Center, College of Basic Medical Science, Jilin University, Changchun, Jilin 130021, P.R. China

Received March 26, 2018; Accepted October 29, 2018

DOI: 10.3892/mmr.2018.9681

Abstract. Diabetic cardiomyopathy is one of the major complications of diabetes, and due to the increasing number of patients with diabetes it is a growing concern. Diabetes-induced cardiomyopathy has a complex pathogenesis and histone deacetylase-mediated epigenetic processes are of prominent importance. The olfactory bromodomain-containing protein 4 (BRD4) is a protein that recognizes and binds acetylated lysine. It has been reported that the high expression of BRD4 is involved in the process of cardiac hypertrophy. The aim of the present study was to investigate the function of BRD4 in the process of high glucose (HG)-induced cardiac hypertrophy, and to clarify whether epigenetic regulation involving BRD4 is an important mechanism. It was revealed that BRD4 expression levels were increased in H9C2 cells following 48 h of HG stimulation. This result was also observed in a diabetic rat model. Furthermore, HG stimulation resulted in the upregulation of the myocardial hypertrophy marker, atrial natriuretic peptide, the cytoskeletal protein α-actin and fibrosis-associated genes including transforming growth factor-β, SMAD family member 3, connective tissue growth factor and collagen, type 1, α1. However, administration of the specific BRD4 inhibitor JQ1 (250 nM) for 48 h reversed this phenomenon. Furthermore, protein kinase B (AKT) phosphorylation was activated by HG stimulation and suppressed by JQ1. In conclusion, BRD4 serves an important role in the pathogenesis of HG-induced cardiomyocyte hypertrophy through the AKT pathway.

Correspondence to: Professor Yan Meng, Department of Pathophysiology, Prostate Diseases Prevention and Treatment Research Center, College of Basic Medical Science, Jilin University, 126 Xinmin Street, Changchun, Jilin 130021, P.R. China
E-mail: mengyan@jlu.edu.cn

Key words: bromodomain-containing protein 4, high glucose, cardiac hypertrophy, atrial natriuretic peptide, JQ1

Introduction

Diabetes mellitus is a metabolic disease caused by a variety of factors and is characterized by elevated blood sugar. In previous years, the incidence of diabetes has consistently increased year upon year, with the number of patients globally predicted to reach 300 million by 2030 (1,2). The resulting fundamental harm is caused by a variety of issues (3-5), with cardiovascular complications being the most prevalent (6). Compared with non-diabetic patients with heart failure, diabetic patients with heart failure have demonstrated worse cardiac function and higher mortality rates (7).

Diabetic cardiomyopathy exhibits a number of notable structural features in the myocardium, with myocardial hypertrophy being the most prominent and typified by an increased cell surface area and the upregulation of atrial natriuretic peptide (ANP) (2). Myocardial hypertrophy is not only a chronic compensatory process but also the main mechanism resulting in the worsening of diabetic cardiomyopathy and risk of heart failure (7).

The pathogenesis of diabetic cardiomyopathy involves multiple signaling cascades, including the c-myc, 5' AMP-activated protein kinase (AMPK) and mechanistic target of rapamycin (mTOR) pathways (1,8-10). Thus, diabetic cardiomyopathy cannot be controlled through the regulation of a single pathway (11). Methylation and histone modifications serve an important role in the process of cell damage in the cardiovascular and central nervous systems (1,12,13). Histone acetylation induces the opening of the chromatin to activate the transcription of *MYC* and nuclear factor-κβ, which are crucial in the process of cardiac hypertrophy (1,12-17). Based on these theoretical foundations, the present study aimed to investigate the potential underlying mechanisms of epigenetics in the development of diabetic cardiomyopathy.

Bromodomain-containing protein 4 (BRD4) is a protein that recognizes and binds acetylated lysine, and promotes transcription by binding to the transcription initiation regions of relevant genes (18). At the same time, it has been reported that the high expression of BRD4, as the upstream gene of c-myc, is involved in cardiac hypertrophy (1,18,19). JQ1, a specific BRD4 inhibitor, has a notable effect in tumor therapy

and transverse aortic constriction (1,20-22). The aim of the present study was to investigate the effect of this inhibitor on the hypertrophy of cardiomyocytes during high glucose (HG)-induced cardiac hypertrophy, to clarify whether epigenetic regulation involving BRD4 is the main mechanism of cardiac hypertrophy (1,23-25).

Materials and methods

Cell culture, treatments and reagents. H9C2, an embryonic rat heart-derived cell line (Shanghai Bioleaf Biotech Co., Ltd., Shanghai, China) was cultured in Dulbecco's modified Eagle's medium (DMEM; Gibco; Thermo Fisher Scientific, Inc., Waltham, MA, USA) containing 5.5 mmol/l D-glucose and supplemented with 10% fetal bovine serum (Clark Bioscience, Richmond, VA, USA), 100 U/ml penicillin and 100 mg/ml streptomycin. In the HG-treated group (HG), cells were incubated in DMEM containing 20 and 30 mmol/l glucose. Control cells were incubated in DMEM containing 5.5 mmol/l D-glucose. JQ1 was purchased from Selleck Chemicals (Houston, TX, USA). Following the pretreatment of cardiomyocytes with 5.5 or 30 mM glucose in a 37˚C incubator supplied with 5% CO_2 for 48 h, H9C2 cells were treated with 250 nM JQ1 or DMSO and incubated for 48 h under the same conditions. Experimental groups consisted of: i) Normal glucose (NG), ii) HG (30 mM glucose) and iii) HG (30 mM glucose) + JQ1 (250 nM). After 48 h of treatment, the cells were photographed under a light microscope (Olympus Corporation, Tokyo, Japan), and the image analysis software Image J version 1.6.0 (National Institutes of Health, Bethesda, MD, USA) was used for the objective analysis of the cell area.

Animal studies. Wistar rats (n=16, male, 160-180 g) were obtained from the College of Pharmacy of Jilin University (Changchun, China). Animal experiments were ethically approved by the Animal Ethics Committee of Jilin University and were in accordance with the regulations of the Institutional Committee for the Care and Use of Laboratory Animals of the Experimental Animal Center of Jilin University. Rats were housed under a 12-h light/dark cycle in an air-conditioned room at 22±2˚C and 45-55% humidity with free access to food and water. Rats were randomly divided into a normal group (n=8) and a diabetes model group (DM; n=8) following adaptive feeding with standard experimental rat chow for one week. Subsequently, the DM group was intraperitoneally injected with streptozotocin (STZ; 30 mg/kg; Sigma-Aldrich; Merck KGaA, Darmstadt, Germany) dissolved in citric acid buffer, while the control group was intraperitoneally injected with the same volume of buffer. After 1 week, blood was collected from the tail vein to test blood glucose levels using a blood glucose meter (BeneCheck, Taiwan, China) and the body weight of the rats was recorded every week. After 8 weeks, the rats were euthanized by excessive intraperitoneal injection of barbiturates (Pentobarbital; 40 mg/kg; Spofadental A.S, Prague) and excised heart tissue was prepared for analysis.

Reverse transcription-quantitative polymerase chain reaction (RT-qPCR). Total RNA was extracted from H9C2 cells and rat myocardial tissues using TRIzol reagent (Invitrogen; Thermo Fisher Scientific, Inc.). RNA samples were converted to cDNA using a Reverse Transcription kit (Vazyme, Piscataway, NJ, USA) according to the manufacturer's protocol. RT-qPCR was performed on an EDC-800 Instrument (Dong Sheng Biotech Co., Ltd., Gunagzhou, China). Briefly, the PCR reaction mix (final volume, 25 μl) consisted of 2 μl cDNA, 2 μl primers, 12.5 μl 2X Power Tap PCR Master Mix and 6.5 μl ddH_2O. The PCR thermocycling conditions and primer sequences are presented in Tables I and II, respectively. PCR was performed on PCR amplifiers (Takara Bio, Inc., Otsu, Japan) and the relative quantities of each mRNA were calculated using agarose gel electrophoresis and a Gel Imaging System (Tanon Science and Technology Co., Ltd., Shanghai, China), and relative gene expression data were analyzed using qPCR and the $2^{-\Delta\Delta Cq}$ method with GAPDH used as an internal control (26).

Western blot analysis. Following treatment, cells and tissues, which were frozen in liquid nitrogen, were harvested and lysed using RIPA buffer (Boston BioProducts, Inc., Worcester, MA, USA) for 30 min at 4-8˚C. Proteins were detected and quantified using a Bio-Rad Protein assay and microplate reader (Bio-Rad Laboratories, Inc., Hercules, CA, USA). Protein samples (30-60 μg) were separated using 12% SDS-PAGE and transferred to polyvinylidene fluoride membranes. Nonspecific binding was blocked using 5% low-fat milk in Tris-buffered saline with Tween-20 (10 mmol/l Tris-HCl, pH 7.5, 200 mmol/l NaCl and 0.05% Tween-20) at room temperature (RT) for 2 h. Subsequently, the membranes were incubated overnight at 4˚C with the following primary antibodies: Rabbit monoclonal anti-ANP (1:500; cat no. C0917; Santa Cruz Biotechnology, Inc., Dallas, TX, USA), rabbit monoclonal anti-BRD4 (1:1,000; cat no. ab128874; Abcam, Cambridge, UK), rabbit polyclonal anti-c-myc (1:1,000; cat no. 10828-I-AP; ProteinTech Group, Inc., Chicago, IL, USA), rabbit monoclonal anti-protein kinase B (AKT; 1:1,000; cat no. 60203-I-Ig; ProteinTech Group, Inc.), rabbit polyclonal anti-phosphorylated-AKT (1:1,000; cat no. ARG51559; Arigo biolaboratories Corp., Taiwan) and mouse monoclonal anti-β-actin (1:5,000; cat no. 66009-I-Ig; ProteinTech Group, Inc.). Then the membranes were incubated for 1 h at RT with secondary antibodies including goat anti-rabbit (1:1,000; cat no. 10828-I-AP; ProteinTech Group, Inc., Chicago, IL, USA) and goat anti-mouse (1:1,000; cat no. 10828-I-AP; ProteinTech Group, Inc.). Electrochemiluminesence color liquid (1:1; Thermo Fisher Scientific, Inc.) was used on a gel image processing system with (Tanon Science and Technology Co., Ltd.) to scan images for statistical analysis using SPSS version 17.0 software (SPSS, Inc., Chicago, IL, USA).

Immunocytochemistry. The hearts of the rats (euthanized as mentioned above) were excised prior to washing with cold phosphate buffered saline (PBS) using filter paper suction to remove residual blood, fat and other non-myocardial tissues. They were weighed and then immediately fixed in 4% paraformaldehyde solution for at least 4 h at RT, followed by dehydration, dipping in wax and paraffin embedding for the preparation of paraffin sections. Excess sections were prepared for subsequent Masson's trichrome staining and haemotoxylin and eosin (H&E) staining. The sections (0.2 mm) were incubated with 2% bovine serum albumin

Table I. Polymerase chain reaction thermocycling conditions.

Gene	Denaturation	Annealing	Extension	Cycle no.
GAPDH	94˚C for 30 sec	55˚C for 45 sec	72˚C for 30 sec	32
Atrial natriuretic peptide	94˚C for 30 sec	60˚C for 30 sec	72˚C for 30 sec	35
Bromodomain-containing protein 4	94˚C for 30 sec	60˚C for 30 sec	72˚C for 45 sec	40
c-myc	94˚C for 30 sec	55˚C for 45 sec	72˚C for 30 sec	32
Transforming growth factor-β	94˚C for 30 sec	55˚C for 45 sec	72˚C for 30 sec	32
Collagen, type 1, α1	94˚C for 30 sec	55˚C for 45 sec	72˚C for 30 sec	32
Connective tissue growth factor	94˚C for 30 sec	55˚C for 45 sec	72˚C for 30 sec	32
SMAD family member 3	94˚C for 30 sec	58˚C for 45 sec	72˚C for 30 sec	32

Table II. Primer sequences.

Gene	Forward primer sequence	Reverse primer sequence
GAPDH	5'-AGAAGGCTGGGGCTCATTTG-3'	5'-AGGGGCCATCCACAGTCTTC-3'
Atrial natriuretic peptide	5'-GCCGGTAGAAGATGAGGTCA-3'	5'-GGGCTCCAATCCTGTCAATC-3'
Bromodomain-containing protein 4	5'-ACAGCCCCAACAGAACAAAC-3'	5'-GCTGGTTCCTTCTTGCTCAC-3'
c-myc	5'-AAGGGAAGACGATGACGG-3'	3'-TGAGCGGGTAGGGAAAGA-5'
Transforming growth factor-β	5'-GCAACAACGCAATCTATGAC-3'	3'-CCTGTATTCCGTCTCCTT-5'
Collagen, type 1, α1	5'-GTACATCAGCCCAAACCCCAAG-3'	3'-CGGAACCTTCGCTTCCATACTC-5'
Connective tissue growth factor	5'-ACTATGATGCGAGCCAACTGC-3'	3'-TGTCCGGATGCACTTTTTGC-5'
SMAD family member 3	5'-CACGCAGAACGTGAACACC-3'	3'-GGCAGTAGATAACGTGAGGGA-5'

(BSA) for 30 min at RT to block nonspecific binding, and then incubated with rabbit polyclonal anti-c-myc (1:400; cat no. 10828-I-AP; ProteinTech Group, Inc.) for 2 h at RT, followed by incubation with goat anti-rat immunoglobulin G (IgG; 1:400; cat no. SA0000I-I; ProteinTech Group, Inc.) for c-myc visualization for 1 h at RT. Between each incubation step, sections were washed three times with Tris-buffered saline withTween-20 (12.5 mM Tris/HCl, pH 7.6, 137 mM NaCl and 0.1% Tween-20).

Determination of collagen contents by Masson's trichrome staining. Excised hearts were prepared as described above and the sections cut from the resultant paraffin blocks were stained using Masson's trichrome stain (0.01 g/ml) for 3-5 min at RT. The sections were observed under an inverted fluorescence microscope (IX71; Olympus Corporation, Tokyo, Japan).

H&E staining. For H&E staining, H9C2 cells were grown on glass coverslips in the presence of HG with or without JQ1, and then fixed in 4% paraformaldehyde for 30 min at RT. Then, these glass coverslips, in addition to those prepared from the aforementioned heart tissue paraffin blocks, were treated with a H&E stain (0.002 g/ml) for 3-5 min at RT. The sections were observed under an inverted fluorescence microscope (IX71; Olympus Corporation).

Immunofluorescence. Subsequent to counting, cells were grown on glass coverslips in the presence of HG with or without JQ1 for 48 h, and then fixed in 4% paraformaldehyde for 30 min at RT. Slides were then washed three times for 3 min each time with PBS. Then, cells were perforated with 0.5% Triton X-100 (in PBS) for 20 min at RT. Subsequent to washing with PBS three times, serum or BSA was added to the slides for 30 min at RT, and then each slide was dipped in diluted primary anti-α-actin (1:500; cat no. 23660-I-AP; ProteinTech Group, Inc.) and placed in a wet box at 4˚C overnight. The next day, following washing with PBS three times, a diluted green Alexa Fluor 488-conjugated donkey anti-rabbit IgG secondary antibody (1:200; cat no. AS035; ABclonal Biotech Co., Ltd., Woburn, MA, USA) was added to the slides in the wet box and incubated at RT for 1 h. Following washing, Hoechst 33258 at a concentration of 0.5 μg/ml (cat no. 1225A038; Beijing Solarbio Science & Technology Co., Ltd., Beijing, China) was added and slides were incubated at RT in the dark for 5 min to stain the nuclei. Following another wash with PBS, the samples were sealed with glycerol and observed under a fluorescence microscope (Olympus Corporation).

Statistical analysis. Results were expressed as the mean ± standard error of the mean of three independent experiments. The statistical significance of differences between the mean values of groups were determined using SPSS 17.0 software (SPSS, Inc., Chicago, IL, USA), and Student's t-tests were used to compare the differences between two groups. To compare >2 sets, one-way analysis of variance analysis with a Newman-Keuls multiple comparison post-hoc test was conducted. $P<0.05$ was considered to indicate a statistically significant difference.

Results

Diabetic rats present with substantial cardiac hypertrophy and fibrosis. A diabetic model was established by injecting STZ into rats for eight weeks, and then the blood glucose levels of STZ-induced diabetic rats were assessed to determine whether the diabetic model was created successfully. The model group demonstrated significantly elevated blood glucose levels compared with the control group, in addition to a relatively reduced body weight (P<0.05; Fig. 1A and B). Furthermore, the heart tissue of the diabetic rats demonstrated significantly increased protein and mRNA expression levels of ANP compared with the control (P<0.01; Fig. 1C and D, respectively). Next, the morphology of the heart tissue from the DM group was examined using H&E staining. Relative to the control group, hearts from the DM group displayed a different degree of structural abnormalities, including broken fibers, disturbed cellular structures, foci with necrotic myocytes and increased cardiomyocyte transverse cross-sectional areas (Fig. 1E). Myocardial fibrosis was observed using Masson's staining (Fig. 1F) and fibrosis in the DM group was enhanced compared with control group.

Expression of BRD4 and c-myc is higher in STZ-induced diabetic rats. Next, the expression levels of BRD4 and c-myc were examined. The results revealed a significantly higher protein expression level of BRD4 (P<0.05) and c-myc (P<0.01) in the DM group compared with the control group (Fig. 2A). Additionally, a significantly higher expression level of BRD4 (P<0.01) and c-myc (P<0.05) in the DM group compared with the control group was observed at the mRNA level (Fig. 2B). Next, immunohistochemistry was used to examine the expression of c-myc in heart tissue. c-myc expression in the DM group was notably higher compared with that in the control group (Fig. 2C).

High glucose induces H9C2 cell hypertrophy and BRD4 upregulation. Given that the DM animals displayed changes in the expression of BRD4 and c-myc, in addition to changes in the structure of the heart tissue, the present study then attempted to elucidate whether the same phenomenon occurs *in vitro*. The H9C2 cell line was used for this purpose, which is a rat cardiomyocyte line. Compared with normal H9C2 cells, H9C2 cells exposed to different glucose concentrations (20 and 30 mmol/l) demonstrated significantly increased ANP protein expression levels in a dose-dependent manner (P<0.05; Fig. 3A). Furthermore, morphological changes in H9C2 cells were induced by high glucose concentrations, as observed by light microscopy (Fig. 3B). Differences in cell size following data analysis with Image J were most pronounced when the glucose concentration was 30 mmol/l, and were significantly larger compared with the control group (P<0.01; Fig. 3C). Subsequently, western blot analysis was used to examine the expression of BRD4 in the control group and HG group. The results revealed that BRD4 and c-myc expression significantly increased with glucose concentration (P<0.05), and the most significant increase was observed with 30 mmol/l glucose compared with the control group (P<0.01; Fig. 3D). These results indicate that BRD4 may participate in cardiomyocyte hypertrophy.

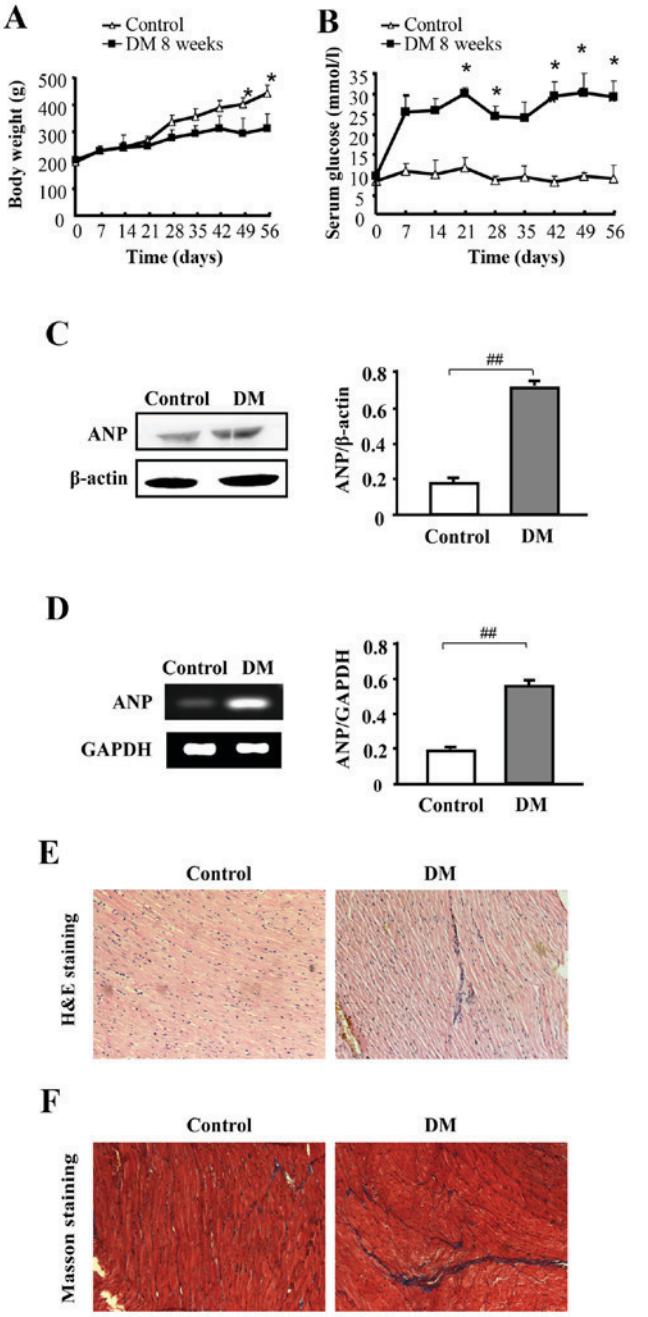

Figure 1. Diabetic rats present with cardiac hypertrophy and fibrosis. Wistar rats were used to simulate a diabetic model by intraperitoneal injections of streptozotocin for 8 weeks (n=8). The ideal diabetic model had fasting-blood glucose levels >12 mmol/l. The control group was treated with vehicle (n=8). (A) Body weight and (B) blood glucose were assessed every week. (C) ANP expression levels in the control and DM groups were analyzed by western blot analysis. (D) mRNA expression levels of ANP in the control and DM groups were examined using reverse transcription-quantitative polymerase chain reaction. (E) H&E staining of the control and DM groups. (F) Masson's staining of the control and DM groups. Scale bar, 50 μm. *P<0.05 vs. the DM group; $^{##}$P<0.01 with comparisons shown by lines. DM, diabetes model; ANP, atrial natriuretic peptide; H&E, haemotoxylin and eosin.

JQ1 significantly inhibits HG-induced cardiac hypertrophy, BRD4 and c-myc expression levels and cardiac fibrosis. A total of 30 mM HG was selected as a suitable concentration for the stimulation of H9C2 cells, and administered JQ1 to observe its effect on the control and HG groups. The results revealed that, compared with the HG

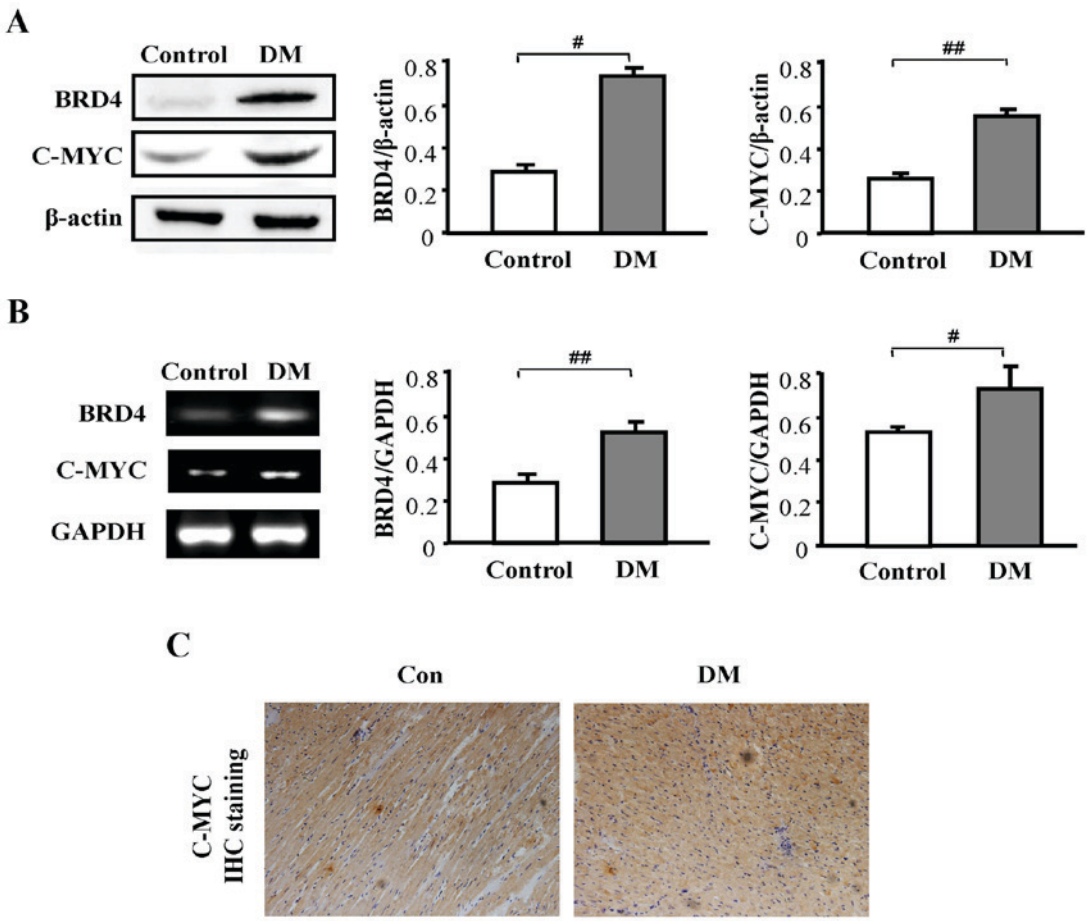

Figure 2. Expression of BRD4 and c-myc is higher in streptozotocin-induced diabetic rats. (A) Protein expression levels of BRD4 and c-myc in the control and DM groups were analyzed using western blot analysis. (B) mRNA expression levels of BRD4 and c-myc in the control and DM groups were examined using reverse transcription-quantitative polymerase chain reaction. (C) IHC analysis of c-myc in the control and DM groups. Scale bar, 50 μm. #P<0.05 and ##P<0.01 with comparisons shown by lines. BRD4, bromodomain-containing protein 4; DM, diabetes model; Con, control; IHC, immunohistochemical.

group, the expression levels of ANP, BRD4 and c-myc were significantly decreased following JQ1 treatment (250 nM) for 48 h (P<0.01; Fig. 4A). RT-qPCR analysis demonstrated a similar significant reduction in mRNA expression levels (P<0.01; Fig. 4B). Representative H&E staining and immunofluorescence images of samples stained with α-actin antibody from the HG group in the absence or presence of JQ1 are presented in Fig. 4C. These results indicated that BRD4 served a function in the process of glucose-induced hypertrophy. As cardiac fibrosis was observed in a large number of diabetic rats, whether HG-induced cardiomyocytes also exhibit this phenomenon was further examined using RT-qPCR. The analysis revealed a significant increase in the expression of the pro-fibrotic genes transforming growth factor-β (TGF-β), connective tissue growth factor, collagen, type 1, α1 and the critical TGF-β mediating factor, SMAD family member 3, in the HG group compared with the control group (P<0.05; Fig. 4D). However, treatment with JQ1 significantly attenuated this HG-induced expression (P<0.05). In general, JQ1 displayed a strong effect on fibrosis induced by high glucose.

HG-induced diabetic cardiomyopathy is mediated through the AKT signaling pathway. To evaluate the underlying mechanism of HG-induced diabetic cardiomyopathy, western blot analysis was performed. As presented in Fig. 5, the AKT pathway was significantly activated under HG stimulation compared with the control (P<0.01); however, JQ1 significantly suppressed this activation (P<0.01).

Discussion

A characteristic of diabetes is high blood sugar, which occurs due to insulin secretion defects, damage from biological effects, or the two combined. Long-term hyperglycemia results in various organ dysfunctions, including that of the eyes, kidneys, heart and blood vessels, in addition to chronic nerve damage, and is associated with the development of heart failure; therefore, diabetes is a major public health problem (7). Diabetic cardiomyopathy has been recognized as a major complication with a characteristic impairment in diastolic function, accompanied by the development of cardiomyocyte hypertrophy, myocardial fibrosis and apoptosis (6,8,10,27,28). Thus, there is an urgent need for novel therapeutic approaches. However, present epidemiological studies of diabetes and treatment management are remain unsatisfactory. Hence, the present research is devoted to the study of diabetic cardiomyopathy.

Emerging data has demonstrated that epigenetic molecules, particularly histone deacetylase, may provide an important mechanism for controlling signaling and gene expression

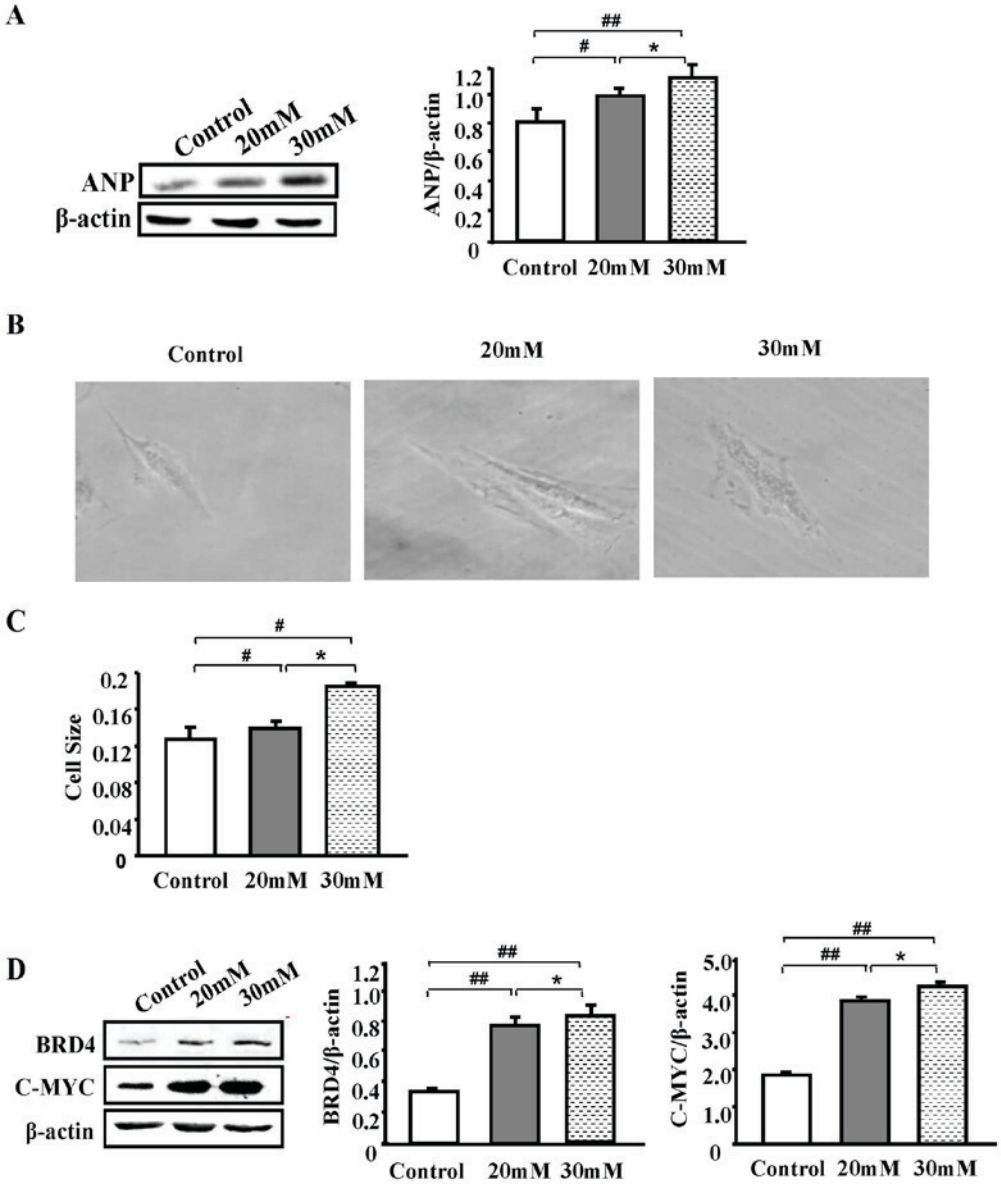

Figure 3. High glucose induces H9C2 cell hypertrophy and upregulates BRD4 expression. (A) Western blot analysis of ANP expression in H9C2 cells subsequent to exposure to different glucose concentrations for 48 h. (B) Comparison of H9C2 cell size following exposure to different glucose concentrations for 48 h under a light microscope. (C) Quantified cell size performed using Image J. (D) Western blot analysis of BRD4 and c-myc expression in H9C2 cells subsequent to exposure to different glucose concentrations for 48 h. Scale bar, 50 μm. *P<0.05, $^{\#}$P<0.05 and $^{\#\#}$P<0.01 with comparisons shown by lines. BRD4, bromodomain-containing protein 4; ANP, atrial natriuretic peptide.

in the heart and kidney. Furthermore, numerous studies have demonstrated that histone deacetylase inhibitors affect pathophysiological processes including myocyte hypertrophy, fibrosis, inflammation and epithelial-to-mesenchymal transition (1,12-15,17,29). Acetylated histones under the control of histone acetyltransferases are recognized by bromodomain and extraterminal domain (BET) proteins, enabling the coordinated regulation of genes involved in cell proliferation, apoptosis and inflammation (1,21,27,30). BRD4, a histone acetylated reader protein, binds to acetylated lysine residues on histone and non-histone proteins to recruit transcriptional regulators, resulting in the activation or repression of gene transcription. It has also been revealed to be involved in various cancer types (20-22,31). Furthermore, a number of studies support the idea that BET family proteins are strongly associated with agonist-dependent cardiac hypertrophy in a mouse model of pressure overload-induced left ventricular hypertrophy (1,19). These results suggest a role for acetyl lysine-binding proteins in the control of pathological cardiac remodeling and lay a strong theoretical basis for the hypothesis for the present study. Understanding the epigenetic mechanisms of glucose-induced myocardial hypertrophy may provide novel therapeutic strategies for reducing heart damage.

Therefore, the aim of the present research was to elucidate the function of BRD4 in diabetes mellitus. First, it was revealed that BRD4 and c-myc expression in the DM group was significantly higher compared with that in the control group (Fig. 2A-C; P<0.05). This suggests that BRD4 is associated with diabetes and confirms the theory that this BET protein is closely associated with cardiac hypertrophy. Next, BRD4 expression was examined *in vitro*. H9C2 cells exposed to different glucose concentrations (20 and 30 mM) demonstrated

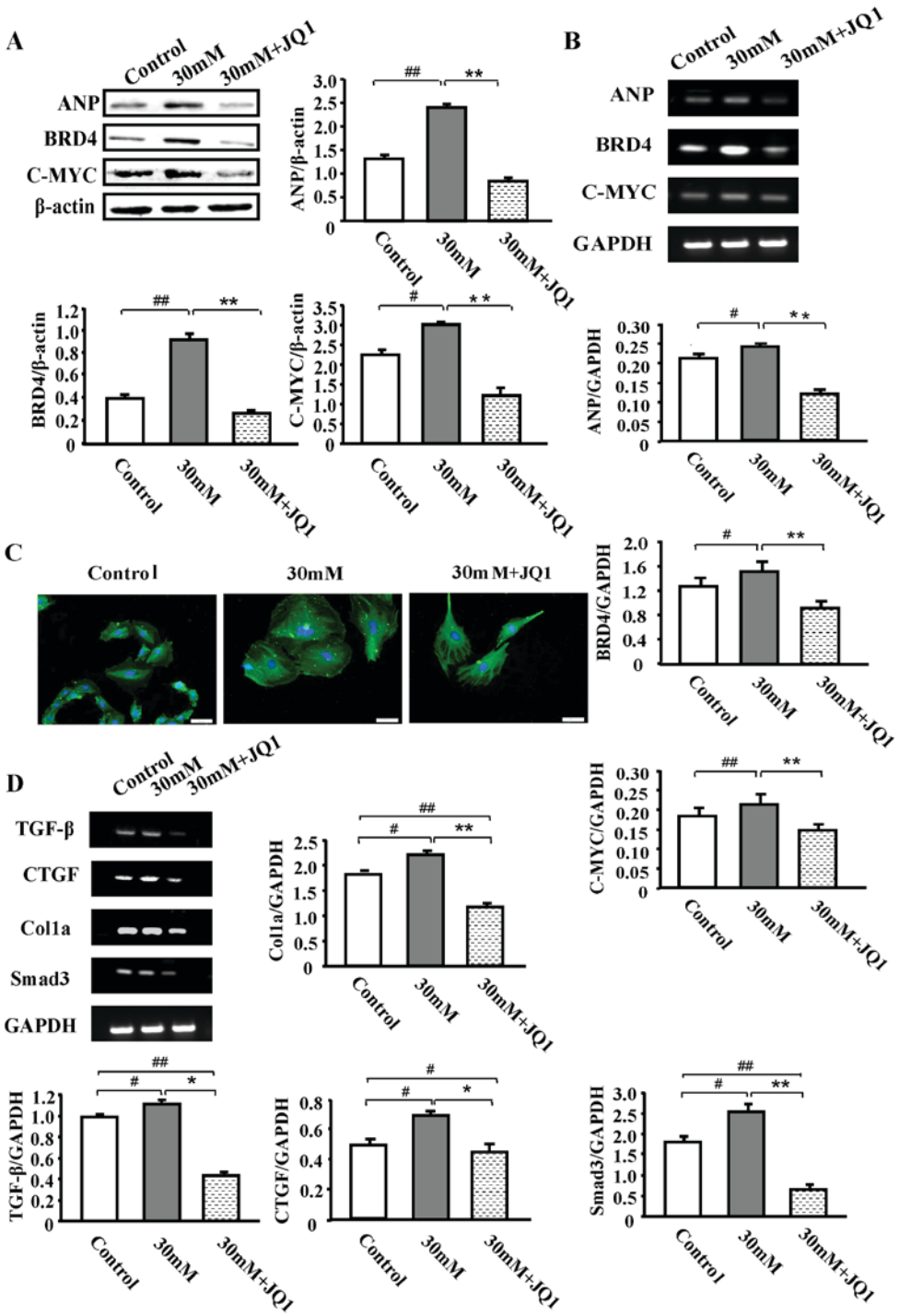

Figure 4. JQ1 significantly inhibits HG-induced cardiac hypertrophy, BRD4 and c-myc expression and cardiac fibrosis. H9C2 cells were treated with 250 nM JQ1 for 48 h after pretreatment with or without HG (30 mmol/l) for 48 h. (A) Western blot analysis of ANP, BRD4 and c-myc protein expression in normal glucose, HG (30 mM glucose) and HG (30 mM glucose) + JQ1 (250 nM) groups for 48 h. (B) RT-qPCR analysis of ANP, BRD4 and c-myc mRNA expression. (C) Images of α-actin staining of untreated H9C2 cells and HG-induced H9C2 cells with or without 250 nM JQ1 treatment for 48 h. (D) mRNA expression levels of fibrosis-associated genes including TGF-β, SMAD3, CTGF and COL1A1 were examined using RT-qPCR. Scale bar, 50 μm. *P<0.05, **P<0.01, $^{\#}$P<0.05 and $^{\#\#}$P<0.01 with comparisons shown by lines. BRD4, bromodomain-containing protein 4; ANP, atrial natriuretic peptide; HG, high glucose; TGF-β, tumor growth factor β; SMAD3, SMAD family member 3; CTGF, connective tissue growth factor; COL1A1, collagen, type 1, α1; RT-qPCR, reverse transcription-quantitative polymerase chain reaction.

high expression levels of ANP, BRD4 and c-myc, similar to the results in the STZ-induced diabetic rats (Fig. 3A and B). BRD4 interacts with positive transcription elongation factor (P-TEFb) in the nucleus through its bromodomain. However, its overexpression results in increased P-TEFb-dependent phosphorylation of the RNA polymerase II (Pol II) C-terminal domain and stimulates transcription *in vivo* (1,30,32). Thus, it was speculated that BRD4, under hypertrophic stimuli, promotes its own recruitment to the transcriptional start site of the gene encoding ANP. The results of the present study validated the idea that 30 mM glucose is an effective inducer of myocardial hypertrophy.

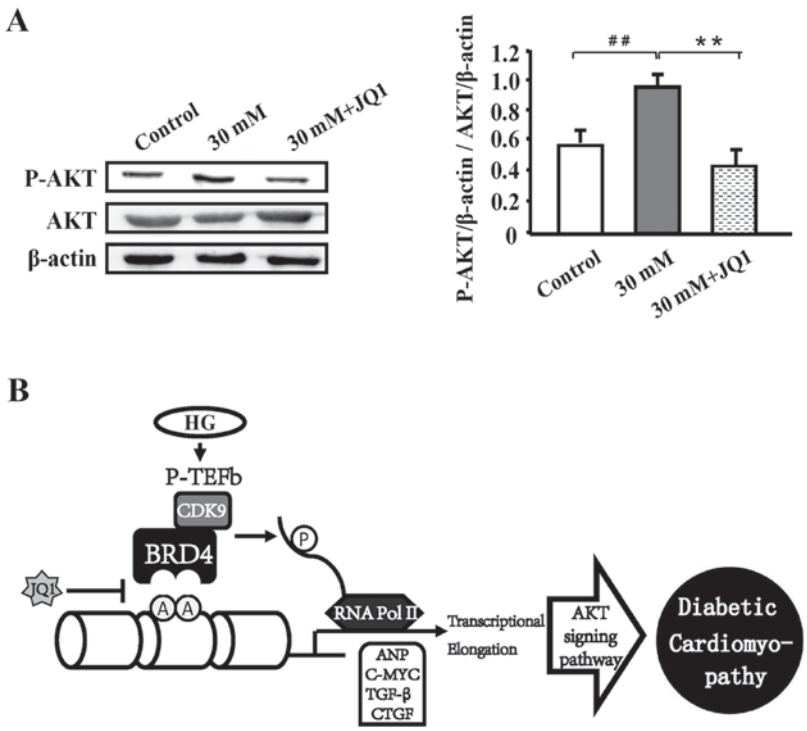

Figure 5. HG-induced diabetic cardiomyopathy occurs through the AKT signaling pathway. (A) Expression levels of P-AKT in the HG group with or without 250 nM JQ1 treatment for 48 h was examined by western blot analysis. (B) A model of the regulation of cardiac hypertrophy by BRD4 under HG stimulation. **P<0.01 and ##P<0.01 with comparisons shown by lines. P-, phosphorylated; AKT, protein kinase B; HG, high glucose; P-TEFb, positive transcription elongation factor; CDK9, cyclin-dependent kinase 9; BRD4, bromodomain-containing protein 4; ANP, atrial natriuretic peptide; TGF-β, tumor growth factor β; CTGF, connective tissue growth factor.

JQ1 is a specific BRD4 inhibitor that binds the bromodomain of BET proteins with high shape complementarity and nanomolar affinity, resulting in the potent, competitive and transient displacement of BRD4 from acetylated chromatin, which causes the suppression of signaling events downstream of Pol II (1,19,21). The present study administered JQ1 to the control and HG groups to examine its effect and to analyze the mechanism by which BRD4 functions. JQ1 significantly inhibited HG-induced cardiac hypertrophy and cardiac fibrosis compared with the HG-alone groups (Fig. 4A-D; P<0.05), in addition to the expression of BRD4 and c-myc.

It has been reported that a single pathway cannot achieve complete control of diabetic cardiomyopathy as it is associated with multiple signaling pathways, including the c-myc, AMPK and mTOR pathways (1,8-11). In the present study, it was demonstrated that a significant decrease in AKT phosphorylation occurred following the administration of a high concentration of glucose (P<0.01), which implies that HG-induced cardiac hypertrophy may be activated through the AKT pathway. Further research of the specific mechanisms and *in vivo* experiments are yet to be performed, but the present study provides a theoretical basis for further clinical research, making JQ1 a potential novel drug for diabetic cardiomyopathy therapy.

The data presented here demonstrated that HG-induced hypertrophy and cardiac fibrosis were associated with BRD4 upregulation. Under hypertrophic stimulus, BRD4 promoted its own recruitment to the transcriptional start site of ANP. However, JQ1 blocked this process (Fig. 4). Additionally, it was discovered that the AKT pathway was activated subsequent to HG stimulation, suggesting that HG-induced cardiac hypertrophy occurs through the AKT pathway, but the effects and molecular mechanism of BRD4 upregulation in cardiac hypertrophy have not been fully elucidated. In conclusion, these data revealed that BRD4 serves a critical role in mediating HG-induced myocardial hypertrophy and cardiac fibrosis, and provides a theoretical basis for the further clinical research of diabetic cardiomyopathy.

Acknowledgements

The authors would like to thank Professor Yan Meng and other teachers from Department of Pathophysiology, Prostate Diseases Prevention and Treatment Research Center, College of Basic Medical Science, Jilin University. The authors also thank H. Nikki March, PhD, from Liwen Bianji, Edanz Editing China (www.liwenbianji.cn/ac), for editing the English text of a draft of this manuscript.

Funding

This study was supported by the Research Fund for the National Natural Science Foundation of China (grant nos. 81370240 and 30900518), the Science and Technology Natural Science Foundation of Jilin Provincial (grant no. 20160101239JC) and the Health Technology Innovation Project of Jilin Province (grant no. 2017J059).

Availability of data and materials

The data used and/or analyzed during the present study are available from the corresponding author on reasonable request.

Authors' contributions

QW, YS and TL conceived and designed the project. QW, YM and LZ participated in the idea of the manuscript. QW, LiaL, YZ and LiyL conducted the cell experiments. QW and YM analysed the data. All authors read and approved the manuscript.

Ethics approval and consent to participate

The present study was approved by the Animal Ethics Committee of Jilin University (approval no. 2016-63).

Patient consent for publication

Not applicable.

Competing interests

The authors declare that they have no competing interests.

References

1. Spiltoir JI, Stratton MS, Cavasin MA, Demos-Davies K, Reid BG, Qi J, Bradner JE and McKinsey TA: BET acetyl-lysine binding proteins control pathological cardiac hypertrophy. J Mol Cell Cardiol 63: 175-179, 2013.
2. Roger VL, Go AS, Lloyd-Jones DM, Benjamin EJ, Berry JD, Borden WB, Bravata DM, Dai S, Ford ES, Fox CS, *et al*: Heart disease and stroke statistics-2012 update: A report from the American Heart Association. Circulation 125: e2-e220, 2012.
3. Gao Q, Guan L, Hu S, Yao Y, Ren X, Zhang Z, Cheng C, Liu Y, Zhang C, Huang J, *et al*: Study on the mechanism of HIF1a-SOX9 in glucose-induced cardiomyocyte hypertrophy. Biomed Pharmacother 74: 57-62, 2015.
4. Manyari DE: Prognostic implications of echocardiographically determined left ventricular mass in the Framingham Heart Study. N Engl J Med 323: 1706-1707, 1990.
5. Rababa'h A, Singh S, Suryavanshi SV, Altarabsheh SE, Deo SV and McConnell BK: Compartmentalization role of A-kinase anchoring proteins (AKAPs) in mediating protein kinase A (PKA) signaling and cardiomyocyte hypertrophy. Int J Mol Sci 16: 218-229, 2014.
6. Liang D, Zhong P, Hu J, Lin F, Qian Y, Xu Z, Wang J, Zeng C, Li X and Liang G: EGFR inhibition protects cardiac damage and remodeling through attenuating oxidative stress in STZ-induced diabetic mouse model. J Mol Cell Cardiol 82: 63-74, 2015.
7. Fukushima A and Lopaschuk GD: Cardiac fatty acid oxidation in heart failure associated with obesity and diabetes. Biochim Biophys Acta 1861: 1525-1534, 2016.
8. Wang Y, Zhang J, Zhang L, Gao P and Wu X: Adiponectin attenuates high glucose-induced apoptosis through the AMPK/p38 MAPK signaling pathway in NRK-52E cells. PLoS One 12: e0178215, 2017.
9. Lin CY, Hsu YJ, Hsu SC, Chen Y, Lee HS, Lin SH, Huang SM, Tsai CS and Shih CC: CB1 cannabinoid receptor antagonist attenuates left ventricular hypertrophy and Akt-mediated cardiac fibrosis in experimental uremia. J Mol Cell Cardiol 85: 249-261, 2015.
10. Langer S, Kreutz R and Eisenreich A: Metformin modulates apoptosis and cell signaling of human podocytes under high glucose conditions. J Nephrol 29: 765-773, 2016.
11. Kim SY, Morales CR, Gillette TG and Hill JA: Epigenetic regulation in heart failure. Curr Opin Cardiol 31: 255-265, 2016.
12. Dekker J and Mirny L: The 3D genome as moderator of chromosomal communication. Cell 164: 1110-1121, 2016.
13. Heinz S, Romanoski CE, Benner C and Glass CK: The selection and function of cell type-specific enhancers. Nat Rev Mol Cell Biol 16: 144-154, 2015.
14. May D, Blow MJ, Kaplan T, McCulley DJ, Jensen BC, Akiyama JA, Holt A, Plajzer-Frick I, Shoukry M, Wright C, *et al*: Large-scale discovery of enhancers from human heart tissue. Nat Genet 44: 89-93, 2011.
15. Phillips JE and Corces VG: CTCF: Master weaver of the genome. Cell 137: 1194-1211, 2009.
16. Schmitt AD, Hu M, Jung I, Xu Z, Qiu Y, Tan CL, Li Y, Lin S, Lin Y, Barr CL and Ren B: A compendium of chromatin contact maps reveals spatially active regions in the human genome. Cell Rep 17: 2042-2059, 2016.
17. Wamstad JA, Alexander JM, Truty RM, Shrikumar A, Li F, Eilertson KE, Ding H, Wylie JN, Pico AR, Capra JA, *et al*: Dynamic and coordinated epigenetic regulation of developmental transitions in the cardiac lineage. Cell 151: 206-220, 2012.
18. Sun Y, Huang J and Song K: BET protein inhibition mitigates acute myocardial infarction damage in rats via the TLR4/TRAF6/NF-κB pathway. Exp Ther Med 10: 2319-2324, 2015.
19. Mumby S, Gambaryan N, Meng C, Perros F, Humbert M, Wort SJ and Adcock IM: Bromodomain and extra-terminal protein mimic JQ1 decreases inflammation in human vascular endothelial cells: Implications for pulmonary arterial hypertension. Respirology 22: 157-164, 2017.
20. Zhang HP, Li GQ, Guo WZ, Chen GH, Tang HW, Yan B, Li J, Zhang JK, Wen PH, Wang ZH, *et al*: Oridonin synergistically enhances JQ1-triggered apoptosis in hepatocellular cancer cells through mitochondrial pathway. Oncotarget 8: 106833-106843, 2017.
21. Mio C, Conzatti K, Baldan F, Allegri L, Sponziello M, Rosignolo F, Russo D, Filetti S and Damante G: BET bromodomain inhibitor JQ1 modulates microRNA expression in thyroid cancer cells. Oncol Rep 39: 582-588, 2018.
22. Wang H, Hong B, Li X, Deng K, Li H, Yan Lui VW and Lin W: JQ1 synergizes with the Bcl-2 inhibitor ABT-263 against MYCN-amplified small cell lung cancer. Oncotarget 8: 86312-86324, 2017.
23. Huynh K, Bernardo BC, McMullen JR and Ritchie RH: Diabetic cardiomyopathy: Mechanisms and new treatment strategies targeting antioxidant signaling pathways. Pharmacol Ther 142: 375-415, 2014.
24. Owen DJ, Ornaghi P, Yang JC, Lowe N, Evans PR, Ballario P, Neuhaus D, Filetici P and Travers AA: The structural basis for the recognition of acetylated histone H4 by the bromodomain of histone acetyltransferase gcn5p. EMBO J 19: 6141-6149, 2000.
25. Bennett RL and Licht JD: Targeting epigenetics in cancer. Annu Rev Pharmacol Toxicol 58: 187-207, 2018.
26. Livak KJ and Schmittgen TD: Analysis of relative gene expression data using real-time quantitative PCR and the 2(-Delta Delta C(T)) method. Methods 25: 402-408, 2001.
27. Perry MM, Durham AL, Austin PJ, Adcock IM and Chung KF: BET bromodomains regulate transforming growth factor-β-induced proliferation and cytokine release in asthmatic airway smooth muscle. J Biol Chem 290: 9111-9121, 2015.
28. Johnson R, Dludla P, Joubert E, February F, Mazibuko S, Ghoor S, Muller C and Louw J: Aspalathin, a dihydrochalcone C-glucoside, protects H9c2 cardiomyocytes against high glucose induced shifts in substrate preference and apoptosis. Mol Nutr Food Res 60: 922-934, 2016.
29. Zhang Y, Babcock SA, Hu N, Maris JR, Wang H and Ren J: Mitochondrial aldehyde dehydrogenase (ALDH2) protects against streptozotocin-induced diabetic cardiomyopathy: Role of GSK3β and mitochondrial function. BMC Med 10: 40, 2012.
30. Duan Q, McMahon S, Anand P, Shah H, Thomas S, Salunga HT, Huang Y, Zhang R, Sahadevan A, Lemieux ME, *et al*: BET bromodomain inhibition suppresses innate inflammatory and profibrotic transcriptional networks in heart failure. Sci Transl Med 9: pii: eaah5084, 2017.
31. Ning B, Li W, Zhao W and Wang R: Targeting epigenetic regulations in cancer. Acta Biochim Biophys Sin (Shanghai) 48: 97-109, 2016.
32. Itzen F, Greifenberg AK, Bösken CA and Geyer M: Brd4 activates P-TEFb for RNA polymerase II CTD phosphorylation. Nucleic Acids Res 42: 7577-7590, 2014.